Peer-reviewed version available at Sensors 2019, 19, 3077; doi:10.3390/s19143077

Article

Wireless Readout of Multiple SAW Temperature Sensors

Gudrun Bruckner [1]*, Jochen Bardong [1]

[1] Carinthian Tech Research (CTR AG), 9524 Villach , Austria; gudrun.bruckner@ctr.at; jochen.bardong@ctr.at
* Correspondence: gudrun.bruckner@ctr.at

Abstract:
It is since long known, that SAW devices, resonators as well as delay lines, can be used as passive wireless sensors for physical quantities like temperature and pressure as well as gas sensors or ID-Tags. The sensors are robust, work passively without battery, can be applied at high temperatures and provide a high resolution. Nevertheless, if the devices should be readout wirelessly in an industrial environment, several constraints have to be taken into account, especially when more than one quantity or device needs to be measured at the same time. The paper addresses the challenges that have to be tackled when establishing multi-sensor-wireless-readout for industrial applications. Major issues here are the legal ISM-band regulations, as well as sampling time and costs, which impose severe restrictions to any system design. We describe several design approaches and their constraints. We have successfully designed sensors based on reflective delay lines that allow the parallel readout of four independent temperature sensors in the 2.45 GHz ISM-band. These devices have been fabricated, positively tested and demonstrate the applicability of SAW sensors for industrial applications.

Keywords: SAW; sensors; wireless; delay lines; industrial application

1. Introduction to SAW sensors

SAW (surface acoustic wave) sensors can provide significant advantages in industrial sensing as they can be readout wirelessly, are working absolutely passive and can sustain high temperatures. It has been shown by many groups, that different physical and chemical quantities can be measured with these devices [1-4]. While the sensors themselves allow a very wide span of operation like temperatures from -200°C to 800°C, frequency from 100 kHz to GHz, and various quantities that can be measured, the field becomes significantly narrower if the restrictions given by ISM-band regulations and practical considerations like antenna size, sampling frequency and cost have to be taken into account. If several sensors have to be readout at the same time the limitations add up even further. This paper describes the general design considerations that have to be taken into account if SAW sensors are to be used in industrial applications and demonstrates a successful example for a wireless multi temperature sensor readout.

The following introduction is intended for readers not familiar with the field of SAW sensors. It should help users to understand the features and constraints of these devices and assist in selecting the right technology for their application.

A general introduction to SAW devices can be found in [5-7]. Sensing with SAW devices is described in [1,8], resonators in [9,10], delay lines in [11,12] and reader units in [13,14].

SAW sensor can be divided into two groups: resonators and delay lines. Resonators as resonant devices show a narrow signal in frequency domain with peaks at their resonance frequency and its corresponding anti-resonance. The higher the quality factor the narrower the peak(s). A sensor effect like temperature or pressure shifts this peak maximum in frequency which can then be tracked in the reading device. The measurement is done via the emission of an electromagnetic radio frequency (RF) wave by a reader unit. The wave is received by an antenna connected with the sensor and

Preprints (www.preprints.org) | NOT PEER-REVIEWED | Posted: 20 June 2019 doi:10.20944/preprints201906.0203.v1

Peer-reviewed version available at Sensors 2019, 19, 3077; doi:10.3390/s19143077

converted to a SAW on the piezoelectric substrate of the device by the interdigital transducer (IDT) structure. As propagation time and frequency of the SAW are influenced by the physical effect the device is exposed to (like changes in temperature or mechanical load of the surface), the analysis of these values provides the desired sensor information when the wave is retransmitted to the reader and analyzed there. While the physical principles of wave generation and propagation are the same for resonators and delay lines, the latter are designed as devices with a wide, flat-topped transfer function that maximizes the bandwidth and thus show a very well defined, sharp peak of the impulse response(s) in time domain. Table 1 gives a short comparison of main resonator and delay line properties.

Table 1. Comparison of delay line and resonator SAW sensors

Delay lines	Resonators
Change of delay time is measured : material constant is temperature coefficient of delay (TCD)	Frequency shift is measured: material constant is temperature coefficient of frequency (TCF) = -TCD
Wide band device: sharp peaks in time-domain	High Q- factor needed for sharp peaks in f-domain -> narrow resonance.
Differential measurement is easy due to multi peak design	Differential measurement requires multiple resonators
Wide band operations allows for wide temperature shift	Too wide temperature shifts might shift the sensor's resonance frequency out of the RF-band
Devices are relatively long ~ > 4-6 mm, measurement corresponds to mean value over delay path ~ 2 mm	Resonators can be small and allow point-like measurements
Sophisticated phase tracking required	High resolution frequency reading needed

The change of the peak position in frequency or time due to temperature changes is described by the temperature coefficient of frequency (TCF) and delay (TCD), respectively. Generally TCF= -TCD for a given material. In the following discussion temperature is used as an example but equivalent considerations can be made for any measurand (e.g. pressure, strain, mass loading).

The delay time t at a given temperature T is calculated relative to the delay time at the reference temperature T_0 in a quadratic approximation as

$$t(T)=t(T_0)\cdot(1+TCD_1\cdot(T-T_0)+TCD_2\cdot(T-T_0)^2). \qquad (1)$$

For sensing applications the linear TC (temperature coefficient) should be big to gain a large sensing effect and hence a high resolution. To avoid ambiguities when calculating the temperature from the measured signal shift, the change of delay time must be close to linear within the range of sensor operation. For example a second- or third-order characteristic with a turn over point within the temperature range would not allow resolving the correct temperature from the measured shift in delay time. Hence only substrate materials with monotonically in- or decreasing temperature shifts can be applied for sensor devices. Usually a 2nd order polynomial with very small second order coefficient is desired for SAW sensors. While these considerations may sound trivial, they limit the choice of suitable sensor materials considerably. The quality of piezoelectric substrates for SAW sensors can be described by the coupling coefficient, a measure to describe the conversion efficiency from electromagnetic RF wave to piezomechanical SAW and back, the propagation velocity of the SAW on the material surface, the SAW's amplitude attenuation while travelling over the surface and the TC which, as a material property, describes the change of the propagation velocity under temperature changes. For temperature sensors of course the stability of the material itself against decomposing and against the loss of the piezoelectric effect at high temperatures is an additional prerequisite.

Preprints (www.preprints.org) | NOT PEER-REVIEWED | Posted: 20 June 2019 doi:10.20944/preprints201906.0203.v1

Peer-reviewed version available at Sensors 2019, 19, 3077; doi:10.3390/s19143077

All these properties are described by the material constants and depend strongly on the chosen orientation in the crystal. For most materials a trade-off between optimal temperature stability, high SAW velocity and RF/SAW-coupling has to be found. E.g. most substrates that are stable at very high temperatures (> 800°C) like Lanthanum-Gallium-Silicate (Langasite, LGS) show small coupling coefficients (about 0.2-0.4%) and low SAW velocities, while materials with coupling coefficients of several percent like LithiumNiobate (LN) or LithiumTantalate (LT) are limited in operation to temperatures of about ~ 300°C.

1.1. General design considerations for SAW sensors

Although it might be tempting to project a multi-purpose SAW sensor system, generally speaking, each application requires a dedicated sensor design. For example, the targeted environment (metal, dust, liquids, corrosives, electromagnetic shields, ..) and the available space for the antenna have to be considered as well as the desired readout distance, data-sampling rate and operation frequency. The higher the operation frequency of the system, the smaller the corresponding antennas can be but generally, the energy losses over the transmission path increase as well. For longer reading distances, antennas with higher gain and hence bigger dimensions have to be applied, which is often limited by practical considerations.

2. Multi Sensor Design

The aim of this work was to realize at least four independent SAW temperature sensors which can be readout simultaneously with a single reader antenna, but without letting the four different sensor signals interfere with each other. The operation temperature should be up to 300°C. The mutual temperature difference between the sensor locations can be as high as 250°C. The minimum sampling rate of a readout of all four sensors is about 1 Hz. High temperature gradients are neither expected in space (along the sensor length) nor in time. As the sensors should be applied in free field measurements, ISM regulations have to be observed

The sensors have been designed by careful consideration of material properties and boundary conditions and selection of appropriate substrate and electrode materials. The different design steps are described in detail in the following section and lead to the choice of a reflective delay line design. The devices have been fabricated and investigated experimentally.

The temperature reading is demonstrated by measuring S11-parameters of the sensors with a Vector Network Analyzer (VNA) at different positions within a tube furnace applying various temperature levels between room temperature and 270°C. The data was analyzed with dedicated analysis scripts (MatLab) to retrieve the relevant sensor data like the delay time, phase information at the peak, signal quality; and from them the temperature reading for each sensor was deduced. The main steps of the data analysis are:

- Hanning window on S-parameter data
- inverse Fourier transform (IFFT) of the windowed S-parameters to time domain, with applied zero padding to get 2048 data points for 80 MHz bandwidth (2.4-2.48 GHz) and 8192 points for 320 MHz bandwidth (2.29 – 2.61 GHz), respectively,
- peak time and phase value detection of all twelve sensor peaks,
- assigning the peak data to the individual sensors and
- computing the temperature from the measured delay time and phase value by applying the known TCD coefficients (polynomial of 2nd order) of Lithiumniobate.

The performance in wireless reading was demonstrated applying two different reading systems and setting up different experimental configurations by variation of the reading antennas, cables and reading distance. The obtained data sets were analyzed in terms of signal strength and resolution versus distance.

2.1. Design considerations

Preprints (www.preprints.org) | NOT PEER-REVIEWED | Posted: 20 June 2019 doi:10.20944/preprints201906.0203.v1

Peer-reviewed version available at Sensors 2019, 19, 3077; doi:10.3390/s19143077

As resonator-based sensors impose fewer demands on the coupling coefficient of the substrate and allow the fabrication of small sensor elements, we have at first considered a resonator based design. If four resonators have to be readout simultaneously each one of them must work at a different frequency. This can be achieved by applying FDMA (Frequency Domain Multiple Access) designs as described for example in [15]. When using multiple resonators for temperature sensing purposes in the same antenna readout cone, the temperature-induced frequency shifts of sensors with adjacent center frequencies must not overlap at the maximum mutual temperature difference they are designed for nor can any sensor's center frequency be allowed to move out of the limits of the ISM-band.

A single resonator can be easily designed for the ISM-band at 433 MHz. This low operation frequency would allow using a well-established material like quartz or a high-temperature sustaining material like LGS as piezoelectric SAW substrate. In addition the low frequency means fewer losses in the free field propagation on the substrate and results in relatively wide electrode structures which enhance the temperature stability of the sensors electrodes. But a short calculation applying equation (1) shows that the frequency shift due to temperature results in a shift of the devices' center frequency by several MHz for 300°C even for a low TCF of 30 ppm/°C. As the ISM-band at 433 MHz is only ~ 1.8 MHz wide no feasible temperature sensor can be realized for the wide operation temperature of ~300°C within that ISM-band; especially as any reliable measurements must be done differentially to compensate for the free path effects, which requires two resonators per sensor.

As the coefficient for pressure or strain is much smaller than the temperature effect, pressure and strain measurements can still be performed within the narrow band [16].

The only ISM-band available for wide band sensor applications is the ISM-band at 2.45 GHz that allows an operation between about 2400-2480 MHz. If four resonator sensors have to work within this bandwidth the available frequency range must be divided in a meaningful manner, allowing the resonators to have different working temperatures and considering some safety margins. Hence less than 20 MHz are available for the frequency shift of each sensor. As 2.45 GHz is already an elevated frequency range for SAW devices, the operation requires high performance substrates like LN or LT. These substrates can be applied to temperatures up to ~ 300°C, which is sufficient for the targeted application. LN has a very high TCF of ~ -94 ppm/°C [17] and is hence ideal for temperature measurements. When it comes to the design with LN, a short calculation using TCF and the temperature range of 300°C shows that only one resonator sensor can fit into the 80 MHz bandwidth. One solution could be reducing the temperature range of operation and/or applying substrates with lower TCF. For example a substrate with a TCF of 40 ppm/°C would allow an operation range of 200°C per resonator sensor. One should be aware that while selecting substrates with a lower TCF is possible, such devices may require more sophisticated sensor designs and the sensitivity of the sensor will be reduced as well. Examples of commercially available substrates are LT 42° Y-cut with a TCD of ~ 40 ppm/°C or 36°Y-cut with a TCD of ~ 30 ppm/°C [18], which operate with SSBW (surface skimming bulk waves). For resonator systems, the loss in sensitivity can be compensated by a sufficiently precise frequency measurement (e.g. 5 kHz for a temperature resolution of 0.05°C) but this may induce a longer sampling time and/or additional equipment costs on the reader side [19].

While the frequency shift due to temperature is the same for delay lines, the analysis in time domain and the possible wide bandwidth of the sensor itself lead to a different behavior.

The sketch in Figure 1 demonstrates the different situation when using resonators or delay lines. Both figures show a draft of the expected sensor response in frequency domain in arbitrary units. For resonators each sensor works at a different frequency and if this frequency is shifted out of the band the devices' response cannot be evaluated any more. With delay lines, all sensors can be designed such that they have the needed very wide bandwidth in frequency domain so that an interrogation sweep will always lead to a successful readout. While the center frequency will still be shifted with temperature, the wide bandwidth ensures that the device still reacts sufficiently within the allowed interrogation band. The example below shows a device with a center frequency of almost 2480 MHz at room temperature to allow the frequency to be shifted down by 66 MHz over the whole temperature range. The optimal signal is set to the center of the aimed temperature region, where most of the operation is expected. A simple analytical model which describes the IDT as a sin(x)/x function [6 p89] was used for the plots of the delay lines whereas the resonators as simply indicated as lines.

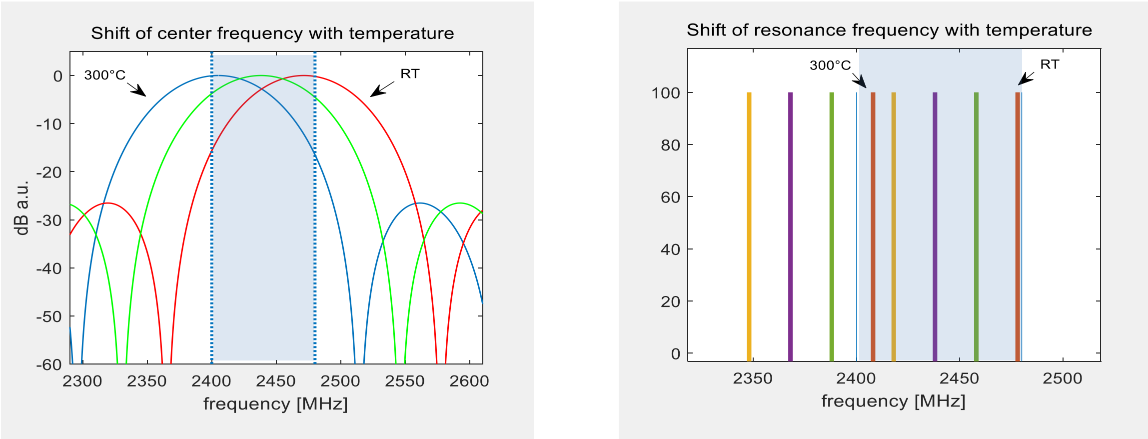

Figure 1. Sketch of frequency shift due to an operation temperature of 300°C with respect to the ISM-band for delay lines and resonators: (**a**) While only a part of the transfer function stays within the band the devices can still be interrogated. The optimal operation point is set toat 150°C. (**b**) Only one resonator (red) stays in the band, but is interfering with 3 other devices. The other devices marked as green, violet and yellow, are completely shifted out of the band.

Following this discussion we have decided to use a delay line design with TDMA (Time Domain Multiple Access) for our sensors. TDMA means that all peaks must be well distinguishable in time domain no matter how the different peaks are shifted by temperature. In addition, the design must be suitable for phase tracking (see “2.2 Phase Analysis” below). Delay lines provide a wider design freedom for the placement of the sensor peaks than resonators as the maximum suitable time is only limited by the propagation losses on the delay line. Practically, the position of the latest peak should be kept below 4 µs for 2.45 GHz devices. We have used a reflective delay line design, as it halves the physical length of the sensor compared to a delay line with two IDTs and needs only one signal port that is connected to the antenna.

As described in the introduction the actual temperature is derived from the shift of the peaks in time domain. If we are considering a delay time of about 2 µs the shift per 0.1 degree is only ~ 20 ps. This resolution cannot be achieved by peak detection in time domain, as the bandwidth is limited to ~80 MHz and hence the distance between the sampling points in time domain is 12.5 ns. Applying signal processing tools like zero padding and parabolic peak fitting to the expected peak the resolution in peak detection can be enhanced depending on the signal to noise ratio. To further increase temperature readout accuracy, especially for weak signals, a phase reading algorithm must be applied to gain the desired resolution of 0.15°C.

2.2. Phase analysis

While the phase value at peak level can be detected within the precision of a few percent within 2π, additional information is required to determine the number of phase rotations and hence determine the most accurate time-shift value possible. This information is provided by measuring the time-shift for delay lines with different lengths. We have studied designs with three and four peaks per sensor at different. One peak serves as a reference for differential measurements, the longest delay line is used for the actual temperature reading and at least one additional short delay line is needed to resolve the phase ambiguity.

Figure 2 shows two different designs based on reflective delay lines that have been fabricated. For both of them an initial delay of at least 1 µs is used to separate the sensor response from pure electric reflections in the propagation path. The actual delay lines for T-reading are 1 µs and 1.4 µs

Preprints (www.preprints.org) | NOT PEER-REVIEWED | Posted: 20 June 2019 doi:10.20944/preprints201906.0203.v1

Peer-reviewed version available at Sensors 2019, 19, 3077; doi:10.3390/s19143077

long. The short delay lines have a length of 100 ns and 130 ns, respectively. After determining the time and phase values at each reflector peak, the temperature can be calculated in two steps: first the time shift of the long delay line is calculated, which allows determining the temperature with an accuracy of better than 10°C. For the short delay line the phase shift stays within one period of 2π for 10°C and hence the accurate temperature can be deduced from the phase reading. This method is only accurate if the temperature is the same for both delay lines. The placement of the short delay line in the middle of the long one allows working with some spacial gradient as long as the mean temperature values of both delay lines are identical. Nevertheless we have finally opted for the second design as we don't expect strong gradients in our application. As the latter design comprises only three peaks, it finally results in a shorter layout and therefore in lower losses. In addition four sensors can be realized at a sensor length of 6 mm whereas only three sensors could be realized with the other design (see Figure 2).

In addition to the two designs described above, many more possibilities can be envisioned. One would be to simply use 3 peaks per sensor and merely arrange the sensors one after the other such that each reflector has its own and unique time position. On the other hand, this would result in very short delay lines and therefore in low resolution. Another possibility that was studied were to modify the first design with four reflectors in a way, that one of the middle reflectors is omitted and the short delay line is not fabricated physically, but represented by the difference of the delay between first and second peak and second and third peak. As one reflector is removed, all the lengths can be reduced so that again 4 sensors can be placed within the chip length of 6 mm. But this design is very sensitive to temperature gradients along the chip length and was hence finally omitted, and we thus finally selected the two designs presented in Figure 2 for fabrication. The sensors have an area of 1.25 mm x 6 mm, comprise a uniformly spaced IDT with a pitch of 0.7 µm and an aperture of 80 times the wavelength. Thus, the center frequency at room temperature is located close to the upper limit of the ISM-band. The devices were processed on LN YZ using an I-Line lithography system, evaporated aluminum as electrode material and mounted into a Kovar housing by Vectron International.

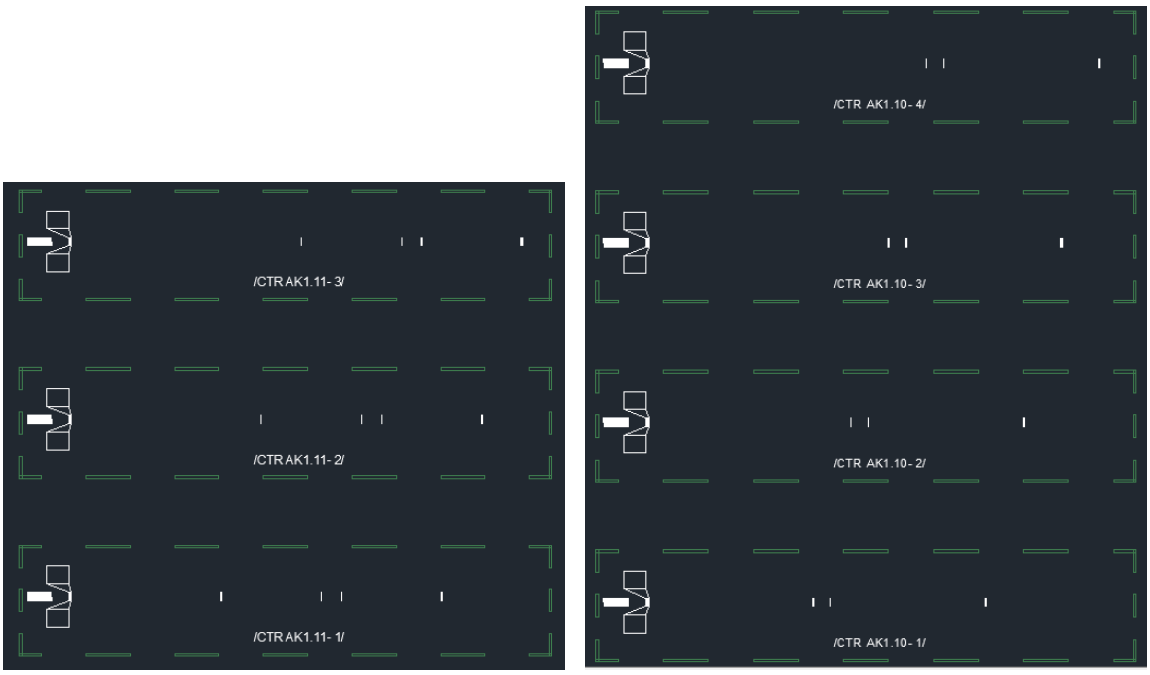

Figure 2. Mask design of two different multi sensor layouts based on reflective delay lines: (**a**) Design A: four peak design for three sensors. (**b**) Design B: three peak design for four different sensors. The IDT structure where the SAW is generated can be seen to the very left of each device where the quadratic wire bond pads are shown as well. The reflectors that correspond to the sensor peaks are visible as short white vertical lines.

3. Results

3.1. Device performance at room temperature

All fabricated devices (3- and 4-peak designs) were measured on wafer level and showed good performance. As expected design B, with 3 peaks per sensor has a slightly better signal-to-noise ratio (SNR) and was selected for further investigation because of the larger number of sensors.

Figure 3 shows the extracted time- and frequency response, measured separately for all four sensors. It can be seen that the frequency response (Fig. 3b) is mostly identical for all sensors while the devices are easily distinguishable in time domain (Fig. 3a). This is exactly as we needed the sensors to work as the frequency response is quite flat during all temperature levels allowing for consistent energy transfer from and to the sensor via the RF link fixed to the 80 MHz of the 2.45 GHz-ISM band and in time domain, each peak can be separated and does not interfere with its adjacent peaks even if one stays at room temperature and its neighbor gets possibly heated up by 250 °C. The IDT's frequency response was designed far wider than the width of the ISM-band to have consistent readouts for the wide temperature shift. The slight asymmetry in the frequency response is typical for the YZ cut of Lithiumniobate IDT transfer functions.

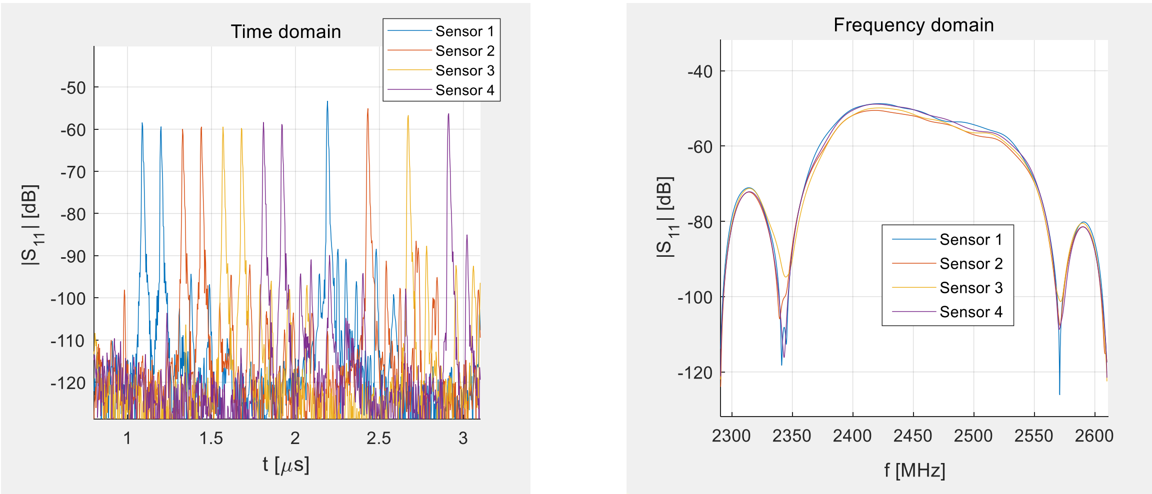

Figure 3. Measured S-parameters of four individual sensors (**a**) left: time domain, the different sensor responses are shown in different colors; (**b**) right: frequency domain, all sensors show the same transfer function – a wideband plateau so that the interrogation in the ISM band can happen successfully no matter of the temperature shift.

Figure 4 demonstrates how the bandwidth of the system influences the width of the sensor peaks in time domain. The blue curve is measured with the full bandwidth of the IDT (320 MHz). This is the way a device as usually analyzed in laboratory. It demonstrates very narrow peaks that can be easily separated from the signals of the other sensors and a good SNR (Signal to Noise Ratio). In comparison to the data shown in Figure 3(a) all four sensors are here measured simultaneously. The red line shows the results if the bandwidth is limited to 80 MHz as allowed for free field measurements and the number of points is reduced to 1024. This low number is applied to make the current S-parameter measurements comparable to the signals a reader can deliver. While no restriction in measurement time was set for the VNA measurement, the reading system should be able to read, analyze and transfer the data to the base station at least a few times per second. This limits the reasonable number of sampling points to about 1024. The yellow curve demonstrates that zero padding to 2048 points before IFFT allows improving the resolution by interpolation of sampling points without increasing the time it takes for a measurement sweep, but only the processing time and the amount of memory needed in the reading system. This method was used during the range measurements described in "3.3 Wireless Reading" and is always applied during a readout-analysis with the reading unit.

Preprints (www.preprints.org) | NOT PEER-REVIEWED | Posted: 20 June 2019 doi:10.20944/preprints201906.0203.v1

Peer-reviewed version available at Sensors 2019, 19, 3077; doi:10.3390/s19143077

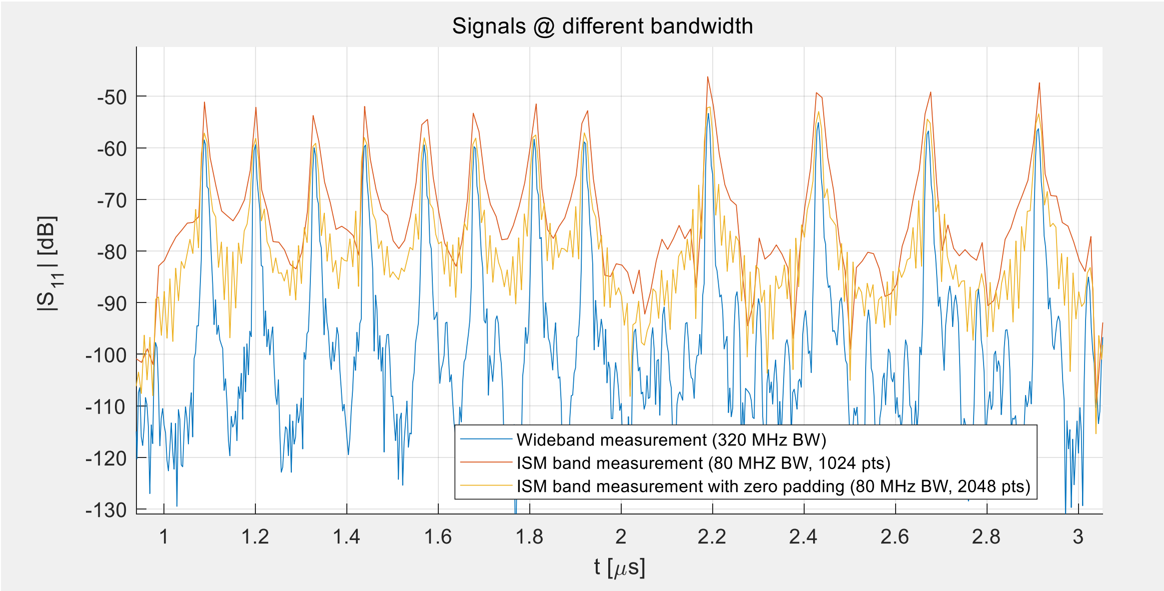

Figure 4. Peaks of the impulse response of the four-sensor-system as measured at different bandwidths at room temperature.

3.2. Temperature measurement

The sensors were installed inside a tube furnace at different distances to the heating coils to create different temperatures. The temperature was increased between 30°C to 270°C in 40°C-steps and held constant at 5 levels for ~ 4 hours each. The measured S-parameters of all sensors were combined and processed by a computer algebra system as described in section 2.

Figure 5 and 6 show selected data taken at different temperatures with a bandwidth of 80 MHz and zero padding of 2048 points. The figures demonstrate the shift of delay time with temperature. Sensor 1 was placed in the middle of the furnace close to two reference sensors (K-type thermocouples), showing considerable time shifts for each temperature level (Fig. 6a), whereas sensor 4 was kept outside of the heated area and is hence hardly influenced by the heating so no time shift is visible (Fig. 6b). Sensors 2 and 3 are placed in between 1 and 4, showing the decreasing heat in lesser time shifts. The temperatures given in the legend of the figures correspond to the temperatures set in the controller of the furnace (marked as set) and the data from the reference sensors and apply only for sensor 1. The other sensors show fewer shifts as they are less heated.

The temperature in the center of the furnace was set to 30°C, 70°C, 110°C, 150°C, 190°C, 220°C and the tube was evacuated to 1 mbar. Each plateau was held for several hours (~4h) to simulate a slow curing process in near thermal equilibrium. The comparison with two reference sensors reveals that the temperature inside the furnace is higher than the set temperature at the controller of the furnace. Especially directly after a heating step, some overshooting of the furnace is visible from the two reference thermocouples. Figure 7 shows the data taken from the four SAW sensors after post processing in a computer algebra system. The TCD value in the data analysis was adjusted to fit to the reference sensor readings. This corresponds to a usual calibration step accounting for slight stresses on the chip due to thermal coefficient of expansion (TCE) mismatch between package, glue and chip, and heat transfer. One can see that sensor 1 follows the temperature curve of the reference perfectly and that all the sensors could be analyzed despite their different temperature regimes and hence time shifts.

 doi:10.20944/preprints201906.0203.v1

Peer-reviewed version available at *Sensors* **2019**, *19*, 3077; doi:10.3390/s19143077

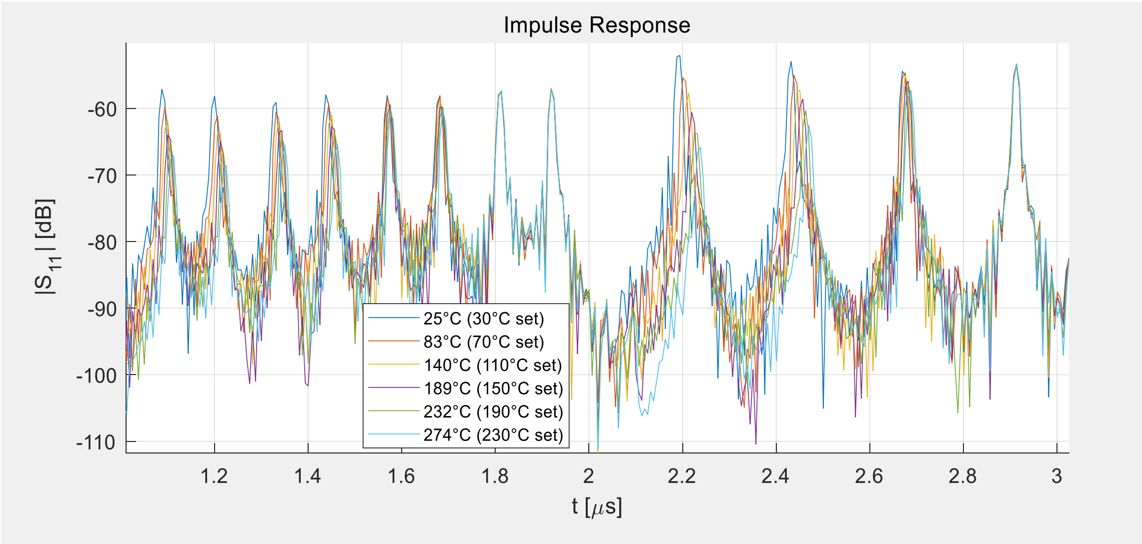

Figure 5. Shift of delay time due to heating of the sensors. Sensor 1 demonstrates the full shift of delay time as it is placed at the center of the furnace, while the other sensors see less and less heat and sensor 4 is practically at room temperature and hence no time-shift occurs.

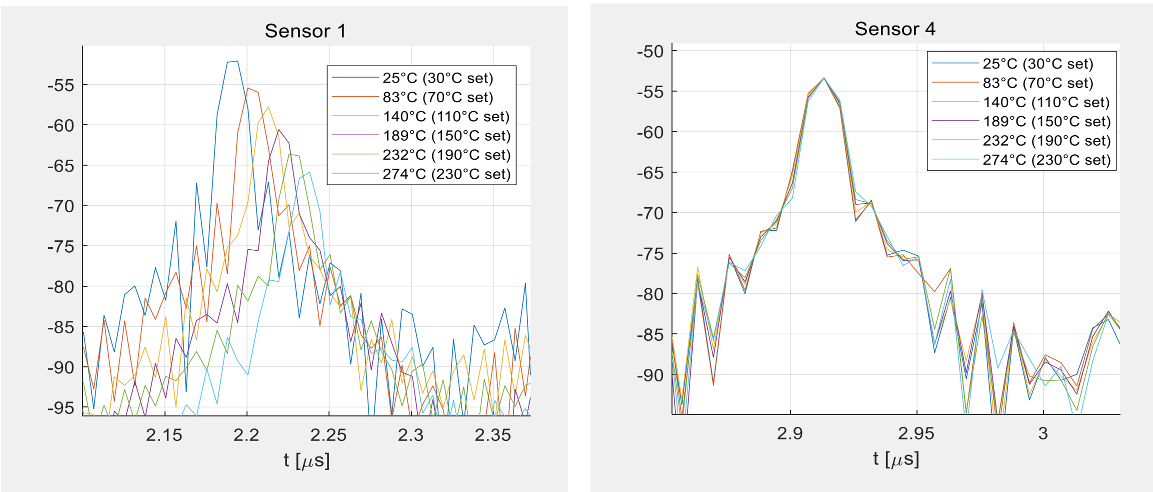

Figure 6. Details of Figure 5 showing the shift of the last peaks of sensor 1(left) and sensor 4 (right)

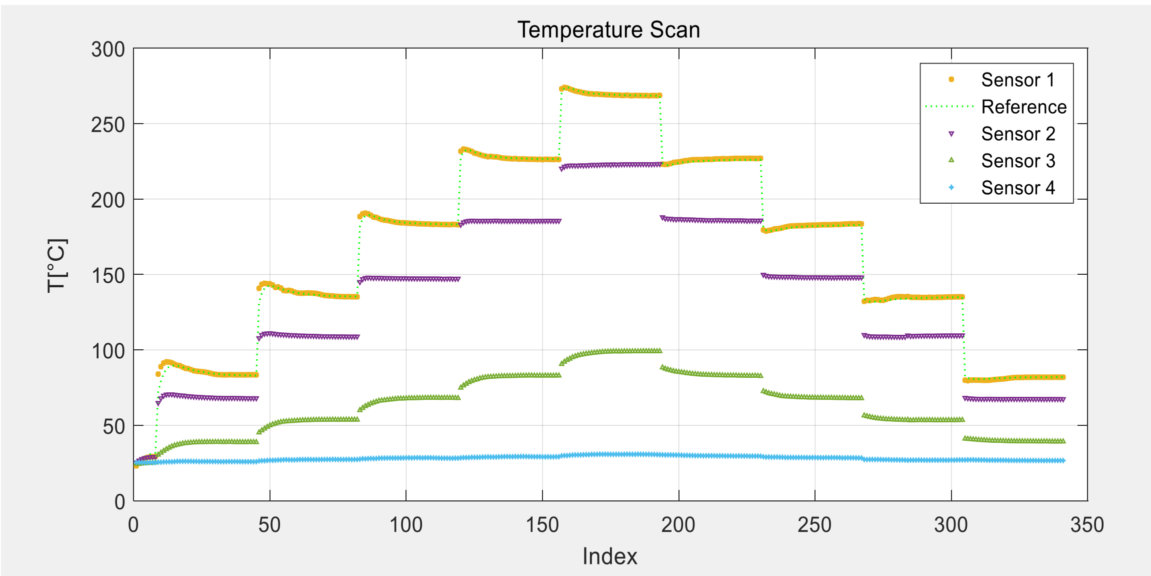

Figure 7. Temperature scans with 4 SAW sensors at different temperatures inside a furnace

3.3. Wireless reading

An extensive study was performed to determine the possible readout distance and resolution of the system when all constraints are applied: band limits 2.4-2.48 GHz, maximum power emitted by the reader system: 10 mW, adapted to the antenna gain, use of metallic slot antennas on sensor side (no PCB prints) for high temperature robustness and several cable lengths between reader unit and reader antenna (print allowed, can be assumed to be located in a somewhat cooler area). These experiments demonstrate the main factors, which affect the system performance in wireless readout:

- emitted power,
- antenna gain and thus size of reading antenna and sensor antenna,
- quality of reader system (sampling frequency and averaging)
    - Switched–Frequency Stepped Continous Wave (S-FSCW),
    - Frequency Modulated Continous Wave (FMCW),
- cables.

As reader units are relatively expensive RF systems, one goal was to access several measurement locations with one reader by 4-fold multiplexing. In combination with the multisensory readout, 16 sensors could be read out with one reader. We have therefore varied the cable length between reader and reading antenna and assessed the achievable reading distance (between sensor and reading antenna) and the resulting resolution.

The sensors are designed for operation in the ISM–band of 2.45 GHz and hence the power for sensor applications is limited to 10 mW. Hence the emitted power must be adjusted according to the gain of the emitting antenna not to exceed this limit. The experiments were performed with two different CTR-readers an S-FSCW and one FMCW. A description of reader principles can be found in [13].

S-FSCW and FMCW require different operation parameters for optimal reading (averaging, amplification). For both readers various cable lengths and antennas have been tested. To make the results comparable, the parameters were set in all configurations so that the emitted power considering antenna gain and losses in the cables did not exceed 10 mW and the sampling frequency of the sensor readout was 5 Hz. All measurements were done using a 9dBi slot antenna on the sensor side.

A two-antenna configuration on the reader side was also tested. Here a high gain (~ 18dBi) antenna was used as receiving antenna(Rx) while the sending antenna (Tx) was kept at 9dBi. Compared to a single 18dBi TxRx setup, the reader output power can be kept higher and about 9dBi are gained in the receiving part.

The phase resolution was measured for the two reader systems as a function of signal amplitude. This data is shown in Figure 8. The given amplitude values are only for comparison and do not give absolute values as they comprise the amplifiers and ADCs in the reader system. The different signal strength was induced by various reading distances and cable lengths. The experiments demonstrate clearly that the achievable resolution depends strongly on the signal amplitude. Because of the different reader architectures and the resulting readout strategies of the two reader types, the main difference between the system performances is mainly because a readout sweep of an S-FSCW unit takes more time than a sweep using a FMCW unit. To be still comparable, an equal sampling rate of 5 Hz was set up for both systems resulting in no averaging for the S-FSCW reader in these experiments, whereas an averaging of 100 was applied for the FWCW. If a slower sampling rate is acceptable, the resolution of the system can be increased by applying higher averaging (see footnote in Table 2).

The measured phase and temperature resolution as a function of antenna distance and the corresponding sensor peak amplitudes are shown in the following tables. The experiments were performed with increasing cable length between reader unit and reading antenna. The cables add losses of ~0.5 dB/m to the system. Different amplitude values occur as longer delay times result in higher attenuation of the peaks. The criterion for the maximum readout distance between reading antenna and sensor antenna was limited by a phase variance of 0.2 rad, which corresponds to a

 doi:10.20944/preprints201906.0203.v1

Peer-reviewed version available at *Sensors* **2019**, *19*, 3077; doi:10.3390/s19143077

temperature resolution of~ 0.15°C. If less resolution is acceptable, a longer reading distance can be achieved.

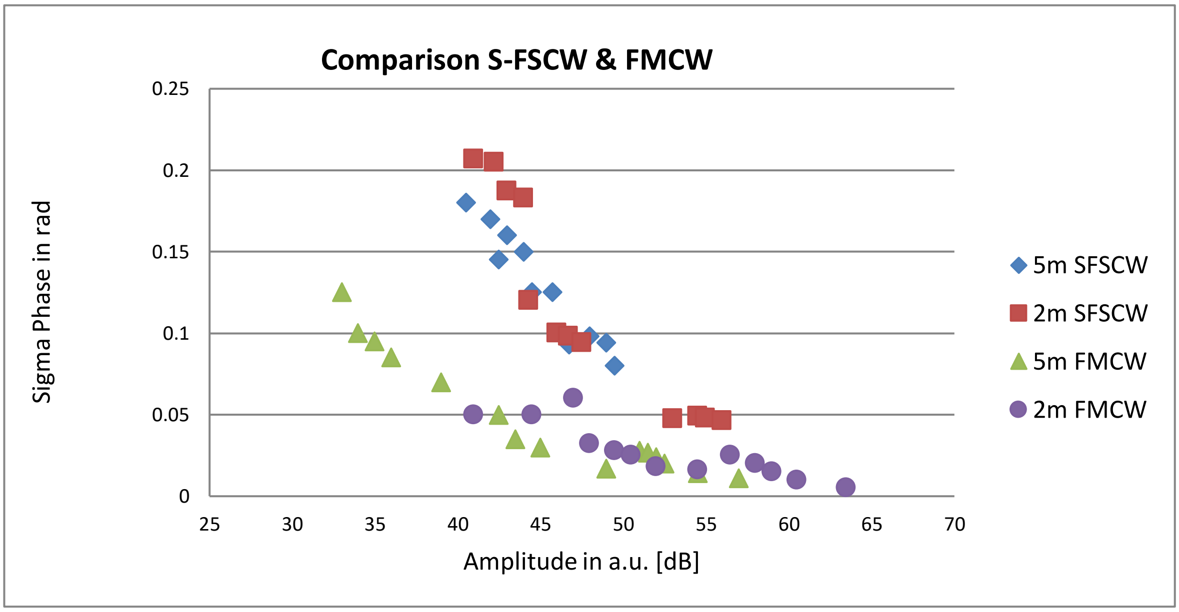

Figure 8. Comparison of the phase resolution of the S-FSCW and FMCW reader as a function of signal strength.

Table 2 gives the results for the S-FSCW system. The largest reading distance can be reached with the shortest reader – antenna – cable. This is understandable as the cable losses in the receiving path cannot be compensated by higher emitted power. The data in Table 3 for the FMCW reader shows similar behavior, with generally better resolution at the same sampling frequency. For both systems the reading distance is limited to around 1 m for the 9dBi antenna or 50 cm for a cable length of 10 m. In all experiments the variance of the phase reading was measured for all peaks. To simplify the display of the data a range of amplitudes is indicated in the tables and only the highest value for the variance is shown. The shown temperature resolution was not measured directly but is calculated from the phase data.

Table 2. Range measurements with S-FSCW reader, averaging =1 and 9 dBi antennas

Cable length [m]	Distance [cm] [1]	Amplitude [dB]	σ_{phase} [rad]	σ_T [°C]
2	50	50-56	< 0.05	<0.04
	100	40-48	< 0.12	<0.09
	120	38-44	< 0.20	<0.14
5	50	45-50	<0.10	<0.07
	100	40-46	<0.15	<0.11
	110	35-43	<0.18	<0.13
10	50	38-40[3]	<0.12[3]	<0.08
	100	---	---	---

[1] Between reader and reading antenna. [2] Between reading antenna and sensor antenna, [3] averaging 10

Longer distances can be achieved with 18dBi antennas especially if a two antenna configuration is used. The reader allows separating transmitting and receiving path. If a smaller antenna with lower gain is used in the emitting path the power can be adjusted to this antenna gain, while the receiving path benefits from the higher susceptibility of the 18dBi antenna. With this configuration the losses within the 10 m of cable can be compensated or the reading distance can be increased to

Peer-reviewed version available at Sensors 2019, 19, 3077; doi:10.3390/s19143077

~2.5 m, resulting in a phase resolution of 0.04 rad for 1m distance and 10 m cable, or 0.13 rad for 2.5 m distance and 2 m cable with the FMCW system.

Table 3. Range measurements with FMCW reader, averaging =100 and 9 dBi antennas

Cable length [m]	Distance [cm] [1]	Amplitude [dB]	σ_{phase} [rad]	σ_T [°C]
2	50	58-62	< 0.025	0.02
	100	42-48	< 0.03	0.02
	140	40-45	< 0.07	0.05
5	50	50-56	<0.02	0.01
	100	43-48	<0.05	0.04
	140	33-40	<0.13	0.09
10	50	30-40	< 5	3.5
	100	---	---	---

[1] Between reader and reading antenna. [2] Between reading antenna and sensor antenna

4. Discussion

The goal of this work was to realize a wireless multi sensor temperature readout based on SAW technology for the operation range from room temperature up to 300°C.

Resonator based solutions have been considered but not implemented, as the band limits of the ISM-band would restrict the sensor performance too much. Instead, wide band delay lines were designed and fabricated to overcome the big frequency shift due to temperature changes. While the bandwidth limits of the ISM-band for the readout system reduce the system resolution in time domain, the layout of the devices was chosen such that it can ensure that the peaks are distinguishable even at big mutual temperature differences between the sensors. We demonstrated a successful simultaneous cable-bound readout of the sensors up to temperatures of ~ 270°C, were the maximum temperature difference of two sensors was ~ 240°C.

Wireless readout performed at room temperature shows that the devices can be interrogated to a distance of about 1 m when 9dBi antennas are applied, the ISM- regulations for "non-specific short range devices" are observed (10 mW) and a harsh criterion of 0.15°C is set for the temperature resolution. Provided that larger antennas can be used or if a lower resolution is acceptable, longer reading distances are possible. The easiest way to increase the readout distance is by simply raising the RF power. This is possible for applications within RF shielded, closed areas or if a special operation permission is granted.

The current SAW sensor chips have a length of ~ 6mm, were ~ 2 mm along the chip surface are used for the temperature reading were the mean value of the temperature within these 2 mm of the delay path is measured. Hence no real point like measurements can be performed.

The design allows only limited use in the presence of steep temperature gradients. The behavior and the limits for such situations where temperature gradients occur should be further investigated as well as the long term temperature stability of the sensors as the sensor material (LN, LT) degrades when exposed to elevated temperatures, especially in chemically reactive atmospheres (e.g. in lab air, NOx, organic carbon based residuals). A possibly way to increase the temperature stability would be to apply a similar design to stoichiometric Lithiumniobate [20].

The sensors demonstrated correct temperature readings at temperatures in the range of 25°C up to 300°C. Finally, this work demonstrates that four individual temperature sensors based on a SAW reflective delay line design can be interrogated at once without interference by a single reader antenna while observing the restrictions of the ISM-band regulations.

Peer-reviewed version available at *Sensors* **2019**, *19*, 3077; doi:10.3390/s19143077

Author Contributions: **Gudrun Bruckner** did the conceptualization of the experiments, the design of the SAW devices, part of the data analysis including MatLab scripts and the preparation of the first draft of the paper as well as the final editing.
Jochen Bardong prepared the experimental setup for the temperature measurements and conducted them, did part of the data analysis and figure preparation and did an extensive review of the paper.

Funding: This project is partly supported within the COMET – Competence Centers for Excellent Technologies - Programme by BMVIT, BMWFJ and the Province of Carinthia and Styria

Acknowledgments: The authors want to thank Alfred Binder (CTR) for the provision of the Kovar packages for the SAW devices, Dominik Holzmann (CTR) for carrying out the range measurements and Vectron International for the processing and packaging of the devices.

Conflicts of Interest: "The authors declare no conflict of interest."

References

1. Reindl, L.M., Scholl, G., Ostertag, T., Scherr, H., Wolff, U., Schmidt, F., Theory and Application of Passive SAW Radio Transponders as Sensors, *IEEE Trans. UFFC* **1998**, *Vol. 45,5*, pp. 1281-1292.
2. Plessky, V.P., Reindl, L.M. Review on SAW RFID tags, *IEEE Trans. UFFC* **2010,** *Vol. 57*, *3*, pp. 654-668.
3. Thiele, J.A., daCunha, M.P., High temperature LGS SAW gas sensor, *Sensors and Actuators B: Chemical* **2006,** *Vol. 113*, *2*, pp. 816-822.
4. Lamothe, M., Plessky, V.P., Friedt, J.-M., Ostertag, T., Ballandras, S., Ultra-Wideband SAW sensors and tags, *IET-EL* **2013**, *Vol. 49, 24*, pp. 1576-1577.
4. Hribisek, M.F., Tosic, D.V., Radosavljevic, M.R., Surface Acoustic Wave Sensors in Mechanical Engineering **2010,** *FME Trans. Vol. 38*, pp. 11-18.
5. Hashimoto, K., Surface Acoustic Wave Devices in Telecommunications, Springer: Berlin, Germany, 2000.
6. Morgan, D.P., Surface-Wave Devices for Signal Processing, Elsevier: New York, U.S.A., 1991, Volume 19
7. Feldmann M., Hénaff, J., Surface acoustic waves for Signal Processing, Artech House: Boston, U.S.A. and London, GB, 1989.
8. Buff, W., SAW sensors, in SAW sensors and Actuators A: Physical **1992,** *Vol. 30,1-2*, pp. 117-121
9. Möller, F., Kuhn, J., Saw resonator temperature sensor **1992.** In Sensors and Actuators A: Physical, *Vol. 30,1-2*, pp. 73-75.
10. Zhgoon, S., Shvetsov, A.S., Sakharov, S.A., Elmazria, O., High-temperature SAW Resonator Sensors: Electrode Design Specifics, *IEEE Trans. UFFC* **2018**, *Vol. 65,4*, pp. 657-664.
11. Steindl, R., Pohl, A., Reindl, L.M., Seifert, F., SAW delay lines for wirelessly requestable conventional sensors, *Proc. IUS* **1998**
12. Reindl, L.M., Ruppel, C.C.W., Berek, S., Knauer, U., Vossiek, M., Heide, P., Oreans, L., Design, fabrication and application of precise SAW delay lines used in an FMCW radar system, *IEEE Trans. on MTT* **2001**, *Vol. 49, 4*, pp. 787-794.
13. Lurz, F., Ostertag, T., Scheiner, B., Weigel, R., Koelpin, A., Reader Architectures for Wireless Surface Acoustic Wave Sensors, Sensors **2018**, 18(6), 1734, In: *Surface Acoustic Wave and Bulk Acoustic Wave Sensors, Spec. Iss.*
14. Plessky, V., Ostertag, T., Kalinin, V., Lyulin, B., SAW-tag system with an increased reading range, *Proc. IEEE IUS* **2010**.
15. Malocha, D.C., et al., A passive Wireless Multi-Sensor SAW Technology Device and System Perspectives, *Proc. Sensors* **2013**, *Vol. 13,5,*pp. 5897-5922.
16. Kalinin, V., Wireless Passive Resonant SAW Sensors for Monitoring Temperature, Strain, Torque and Pressure, *Proc. VIII ECCOMAS Thematic Conference on Smart Structures and Materials, SMART* **2017**.
17. http://www.roditi.com/SingleCrystal/LiNbO3/liNBO3-Properties.html (accessed on 19.6. 2019)
18. http://www.roditi.com/SingleCrystal/Lithium-Tantalate/LiTaO3-Properties.html (accessed on 19.6. 2019)
19. Kalinin, V. Comparison of frequency estimators for interrogation of wireless resonant SAW sensors, *Proc. Joint Conference of IEEE IFCS & EFTF* **2015**, pp. 498-503.
20. Streque, J *et al*., "Stoichiometric Lithium Niobate Crystals: Towards Identifiable Wireless Surface Acoustic Wave Sensors Operable up to 600 °C," in *IEEE Sensors Letters*, vol. 3, no. 4, pp. 1-4, April 2019, Art no. URL: http://ieeexplore.ieee.org/stamp/stamp.jsp?tp=&arnumber=8678851&isnumber=8680794